Shell structure and few-nucleon removal in intranuclear cascade

D Mancusi[1], A Boudard[1], J Carbonell[1], J Cugnon[2], J-C David[1] and S Leray[1]

[1] CEA, Centre de Saclay, IRFU/Service de Physique Nucléaire, F-91191 Gif-sur-Yvette, France
[2] University of Liège, AGO Department, allée du 6 Août 17, bât. B5, B-4000 Liège 1, Belgium

E-mail: davide.mancusi@cea.fr

Abstract. It is well known that intranuclear-cascade models generally overestimate the cross sections for one-proton removal from heavy, stable nuclei by a high-energy proton beam, but they yield reasonable predictions for one-neutron removal from the same nuclei and for one-nucleon removal from light targets. We use simple shell-model calculations to investigate the reasons of this deficiency. We find that a correct description of the neutron skin and of the energy density in the nuclear surface is crucial for the aforementioned observables. Neither ingredient is sufficient if taken separately.

1. Introduction

Nuclear reactions between high-energy ($\gtrsim 150$ MeV) nucleons or hadrons and nuclei are usually described by means of *intranuclear-cascade* (INC) models [1]. In this framework, the projectile is assumed to initiate an avalanche of binary collisions with the nucleons of the target, which can lead to the emission of energetic particles. The nature of INC models is essentially classical. It is typically assumed that nucleons are perfectly localised in phase space and are bound by an average, constant potential; moreover, it is assumed that subsequent elementary collisions are independent.

It was realized some time ago that INC models systematically fail to describe inclusive cross sections for the removals of few nucleons [see e.g. 2, 3]. This is especially surprising in view of the fact that these observables are associated with peripheral reactions and mostly involve collisions between quasi-free nucleons; one would therefore expect intranuclear cascade to provide an accurate description of this particular dynamics. This puzzling result has been known for many years now, but no convincing explanation has ever been put forward.

We will show that the few-nucleon removal process at high energy is sensitive to the the description of the nuclear surface, which we draw from a simple shell-model calculation. We will show that the predictions of an INC model [4] can be substantially improved by casting the shell-model calculation results in a form adaptable to the nuclear model underlying INC.

2. Model description

It is generally assumed that the first stage of high-energy nucleon-nucleus reactions can be described as an avalanche of independent binary collisions. The nuclear model underlying INC is essentially classical, with the addition of a few suitable ingredients that mimic intrinsically

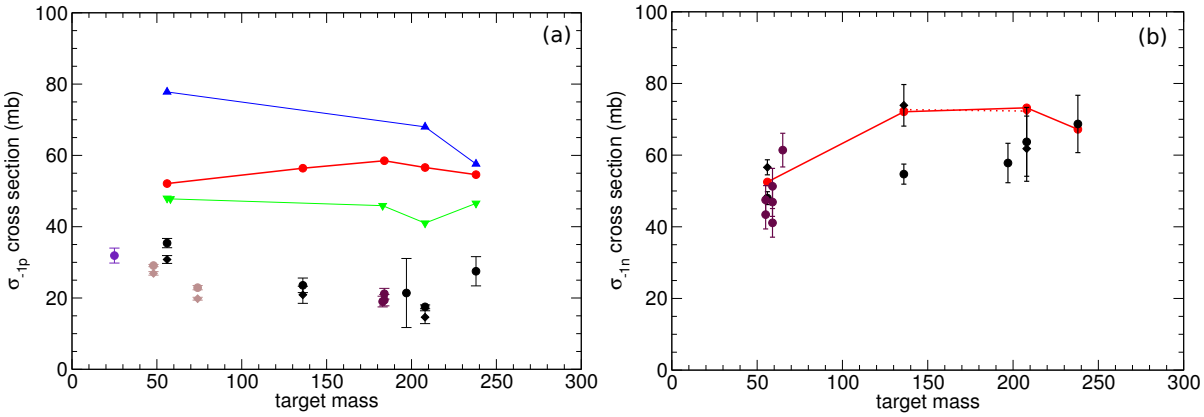

Figure 1. Experimental data for one-proton- (a) and one-neutron-removal cross sections (b) in proton-nucleus reactions above 500 MeV incident energy, as a function of the target mass. Diamonds refer to experimental beam energies around 500 MeV, while circles represent energies between 800 and 1000 MeV. The solid curves represent calculations with INCL (red), Isabel (blue) [9] and Bertini [10] (green) at 1000 MeV. Experimental data taken from Refs. 2, 11–20.

quantum-mechanical features of the initial condition and of the dynamics. At the end of the intranuclear cascade, an excited remnant is left. The de-excitation of this nucleus is typically described by a statistical de-excitation model.

In what follows, we shall make explicit reference to the Liège Intranuclear Cascade model [INCL, 4] and the ABLA07 statistical de-excitation model [5]. The INCL/ABLA07 coupling is in general quite successful at describing a vast number of observables in nucleon-induced reactions at incident energies between ~ 60 and 3000 MeV [6]. The work described hereafter was performed with the latest C++ version of INCL [INCL++, 7].

The INCL model is peculiar in that it explicitly tracks the motion of all the nucleons in the system, which are assumed to move freely in a square potential well. The radius of the well is not the same for all nucleons, but it is rather a function $R(p)$ of the absolute value of the particle momentum (which is a conserved quantity in absence of collisions). The initial particle momenta are uniformly distributed inside a sphere of radius $p_F = 270$ MeV/c. The relation between momentum and radius of the potential well is such that the space density distribution is given by a suitable Saxon-Woods parametrisation; moreover, the nuclear surface is predominantly populated by nucleons whose energy is close to the Fermi energy [8].

3. One-nucleon-removal cross sections

Figure 1 shows the experimental data for one-nucleon removal in proton-induced reactions at energies $\gtrsim 500$ MeV, as a function of the target mass (all targets are β-stable). Calculations with INCL/ABLA07 are shown for comparison. It is clear that the model predictions are in the right ballpark for neutron removal, but they overestimate the proton-removal data by a factor that can be as large as 3–4 for heavy nuclei. Note also that other cascade models similarly overestimate the proton-removal cross sections. Figure 1 suggests that INC models might be affected by a fundamental defect. It is however rather surprising that the deficiency clearly manifests itself in proton removal, but neutron removal seems unaffected.

The analysis of the model calculations indicates that one-proton removal is dominated (about 90% of the cross section) by events with only one proton-proton collision. The two protons leave the nucleus, which however retains some excitation energy. If only one collision took place, the excitation energy is given by the energy of the proton hole, i.e. the difference between the Fermi energy and the energy of the proton that was ejected. This excitation energy is evacuated during

the de-excitation stage by neutron evaporation. If the excitation energy is lower than the neutron separation energy, no particle will be evaporated and the energy will be evacuated as gamma rays; in this case the final (observed) residue will therefore be the target nucleus minus one proton. If the excitation energy allows for neutron evaporation, the final residue will be lighter (target minus one proton minus x neutrons). The one-proton-removal cross sections are therefore extremely sensitive to the excitation energy left in the nucleus after the cascade. Note that there is a subtle difference between one-proton and one-neutron removal. One-neutron removal can be realized in two ways: either as a neutron ejection during INC followed by no evaporation (this is analogous to the proton-removal mechanism), or as no neutron ejection during INC followed by evaporation of one neutron.

Our results are essentially independent of the choice of the de-excitation model, since all of them employ very similar separation energies for stable nuclei. Comparison with the experimental data (Fig. 1) seems to suggest that INC underestimates the excitation energy associated with the ejection of a proton; larger excitation energies would lead to increased neutron evaporation and would therefore reduce the one-proton-removal cross section.

4. Refinement of the INC nuclear model

We mentioned at the end of Section 2 that the nuclear surface is predominantly populated by nucleons whose energy is close to the Fermi energy. The ejection of one such nucleon during INC results in little excitation energy for the cascade remnant. However, even deeply-bound nucleons have a non-vanishing probability to be found in the nuclear surface; this aspect is usually neglected by INC models. Another detail that is usually neglected in the INC picture is the presence of neutron (or proton) skins in certain nuclei, such as ^{208}Pb. For surface reactions, this means that the local neutron density is several times larger than the proton density, leading to an enhanced probability for proton-neutron collisions.

4.1. Shell-model calculations

We have estimated the magnitude of both the effects above with a simple shell-model calculation. We assumed a central Saxon-Woods nuclear potential with a spin-orbit term and a Coulomb term for the protons [21]. We numerically solved the radial part of the Schrödinger equation and determined the eigenfunctions and the eigenvalues of the bound states. The single-particle energies correctly reproduce the energies of the particle-hole states in ^{207,209}Pb and ^{207}Tl,Bi.

We would like to use the shell-model proton and neutron densities as inputs for our INC calculation; however, the particle densities in INCL cannot be given by an arbitrary function, so we must somehow adapt the shell-model densities. We chose to fit them with Saxon-Woods distributions (shown in Fig. 2 as dashed lines). The best-fit parameters show that the shell-model densities exhibit a neutron skin in ^{208}Pb. We have thus decoupled the INCL parameters describing the neutron space density from those describing the proton space density. The proton densities have not been modified (because they are already given by fits to the experimental charge radii), but the neutron parameters have been adjusted by the skin thicknesses resulting from the fit shown in Fig. 2.

We have explained in the previous section that the outcome of single-collision cascades is sensitive to the energy of the ejected nucleon. We assume that the probability that a collision ejects a nucleon from a given shell is proportional to the local density of the shell orbital. Furthermore, we neglect rearrangement of the other nucleons in the Fermi sea after the collision; this amounts to assuming that the excitation energy of the hole is simply given by the depth of the hole, measured from the Fermi energy.

With these assumptions, we can estimate the mean and RMS excitation energies that are left in the nucleus if a hole is punched in the Fermi sea at a certain distance from the center. These

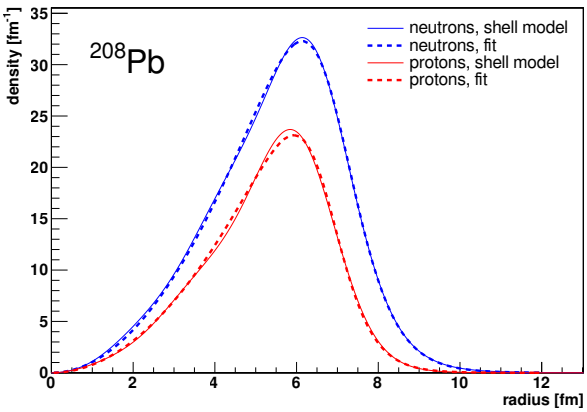

Figure 2. Proton (red) and neutron (blue) densities for ^{208}Pb. The thin solid lines represent the result of the shell-model calculation, while the thick dashed lines are Saxon-Woods fits.

Table 1. Cross sections for one-nucleon removal in 1-GeV p-nucleus reactions, with the following model variants: (a) standard, (b) standard plus neutron skin, (c) standard plus surface fuzziness, (d) standard plus neutron skin and surface fuzziness. Experimental data are taken from Refs. 16, 22.

	^{40}Ca		^{208}Pb	
	$-1p$	$-1n$	$-1p$	$-1n$
(a)	59.8	46.4	59.5	82.1
(b)	58.8	41.4	50.9	112.0
(c)	51.6	38.3	42.1	63.4
(d)	51.9	35.3	33.6	83.8
exp[1]	54.7 ± 7.9	29.8 ± 6.4	17.6 ± 0.5	63.7 ± 9.6

[1] The experimental values for ^{40}Ca refer to an incident energy of 763 MeV.

quantities are plotted in Fig. 3 for the shell-model calculation and for the standard INCL nuclear model ($f = 0$).

It is clear from the results displayed in this picture that the standard INCL nuclear model yields mean and RMS excitation energies that are quite different from those resulting from the shell model. In the surface region, the proton mean and RMS values from INCL are sensibly lower than their shell-model counterparts, which seems to confirm that the excitation energy associated with the ejection of a proton is underestimated by INCL.

4.2. Surface fuzziness

We mentioned in Section 2 that an INCL nucleon moves in a square-well potential whose radius $R(p)$ depends on the nucleon momentum. The function $R(p)$ is uniquely determined by the choice of the space density $\rho(r)$ and by the assumption that nucleon momenta are uniformly distributed in a sharp-surface Fermi sphere. We have shown above that this construction results in excitation energies for one-collision reactions that are much smaller than those resulting from the shell model and, arguably, than those suggested by the available experimental data.

We refine the INCL nuclear model by making $R(p)$ into a random variable. We introduce a *fuzziness parameter* f ($0 \leq f \leq 1$) and a *fuzzy* square-well radius $R(p, f)$. The precise definition of $R(p, f)$ is outside the scope of this short paper, but it has the following properties: first, for $f = 0$ we recover the standard sharp correlation ($R(p, 0) = R(p)$). Second, for given values of p and f, $R(p, f)$ is a random variable that describes the radius of the square well. The fluctuations in $R(p, f)$ are small if f is close to zero and they are large if f is close to one. Moreover, the fluctuations are constructed in such a way that the space density is still given by $\rho(r)$ and the momentum density is still given by a sharp-surface Fermi sphere.

The construction of the refined INCL nucleus is analogous to the standard preparation algorithm [8]. The only difference is that the radius of the square-well potential is no longer in one-to-one correspondence with the nucleon momentum.

The refined nuclear model introduces fluctuations in the space distribution of nucleons with a

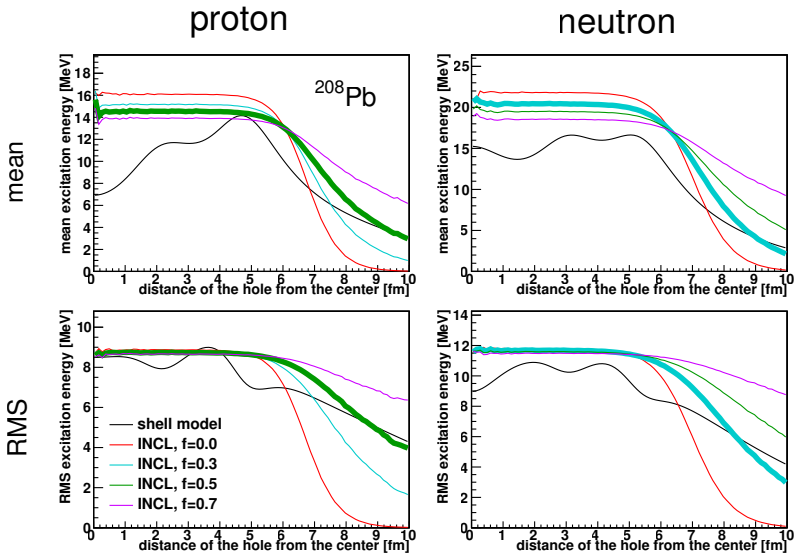

Figure 3. Mean (top) and root-mean-square (bottom) excitation energy induced by the presence of a proton (left) or neutron hole (right) in ^{208}Pb, as functions of the hole position. The black lines represent the shell-model result, while the colored lines are the results generated by the INCL nuclear model for different values of the fuzziness parameter f. The thick lines represent the selected parameter values.

given energy; equivalently, it introduces additional energy fluctuations for the nucleons found at a given position. Figure 3 indeed demonstrates that the average and RMS excitation energies for surface holes *increase* for increasing surface fuzziness, i.e. for increasing fluctuations. No value of the fuzziness parameter yields a good fit to the shell-model result, even if one limits oneself to the surface region. There is some degree of subjectivity in the choice of the best-fit values, which are taken to be $f = 0.5$ for protons and $f = 0.3$ for neutrons. For ^{40}Ca (not shown), the best-fit value was taken to be $f = 0.3$ for both protons and neutrons.

Summarizing, we have refined the INCL nuclear model in two respects. First, we have introduced a neutron skin, as described in Section 4.1. Second, we have introduced surface fuzziness, which increases the energy content of the nuclear surface and the probability for deep-nucleon removal in surface collisions. In the framework of the shell model, this effect is genuinely quantum-mechanical and is due to the penetration of the wavefunction in the classically forbidden region.

5. Results and conclusions

We turn now to the analysis of the results of the refined INC model. Table 1 shows how the neutron skin and the surface fuzziness affect the one-nucleon-removal cross sections in 1-GeV p+^{40}Ca and p+^{208}Pb. Unfortunately, no experimental data are available for p+^{40}Ca at 1 GeV, but since we do not expect a strong dependence on the projectile energy, we can compare to Chen *et al* 's data at 763 MeV [22].

Several observations are due. First, the introduction of the neutron skin in ^{208}Pb boosts the neutron-removal cross section, as expected. This is however undesired, since the cross section calculated by standard INCL is already in moderate excess of the experimental value. Second, surface fuzziness suppresses the cross sections for both one-nucleon-removal channels. This is true both for ^{40}Ca and ^{208}Pb. Third, neither effect is sufficient to compensate for the overestimation of the proton-removal cross section in ^{208}Pb *if considered alone*.

When the two refinements are simultaneously applied to ^{208}Pb, the effect of surface fuzziness for neutron removal almost exactly compensates the effect of the neutron skin, and the final result (83.8 mb) is very close to the value calculated with standard INCL (82.1 mb), which is within two standard deviations (about 30%) of the experimental value. The proton-removal cross section, on the other hand, is reduced by almost a factor of two, which brings it much closer to the experimental data, but not quite in agreement with it. The agreement for the p+^{40}Ca

cross sections is also improved: the change in the proton-removal cross section is minor ($\sim 10\%$) and stays within the experimental error bar, but the neutron-removal cross section is reduced by $\sim 50\%$, in fair agreement with the experimental value.

In conclusion, we have shown that INCL fails to describe the cross sections for one-nucleon removal at high energy. We have used simple shell-model calculations to show that the key to this deficiency lies in the presence of neutron skins in heavy, stable nuclei and in the energy content of the nuclear surface. In the future we will need to generalize our approach to non-magic nuclei and devise a systematic approach to the description of the properties of the nuclear surface.

References

[1] Serber R 1947 *Phys. Rev.* **72** 1114–1115

[2] Jacob N P and Markowitz S S 1975 *Phys. Rev. C* **11**(2) 541–545

[3] Audirac L, Obertelli A, Doornenbal P *et al.* 2013 *Phys. Rev. C* **88**(4) 041602

[4] Boudard A, Cugnon J, David J C, Leray S and Mancusi D 2013 *Phys. Rev. C* **87** 014606 (*Preprint* `1210.3498`)

[5] Kelić A, Ricciardi M V and Schmidt K H 2008 ABLA07 — towards a complete description of the decay channels of a nuclear system from spontaneous fission to multifragmentation *Joint ICTP-IAEA Advanced Workshop on Model Codes for Spallation Reactions* (Trieste, Italy: IAEA) p 181 report INDC(NDC)-0530

[6] Leray S, David J C, Khandaker M, Mank G, Mengoni A, Otsuka N, Filges D, Gallmeier F, Konobeyev A and Michel R 2011 *J. Korean Phys. Soc.* **59** 791–796
IAEA benchmark of spallation models `http://www-nds.iaea.org/spallations`

[7] Mancusi D, Boudard A, Cugnon J, David J C, Kaitaniemi P and Leray S 2014 *Phys. Rev. C* Submitted

[8] Boudard A, Cugnon J, Leray S and Volant C 2002 *Phys. Rev. C* **66** 044615

[9] Yariv Y and Fraenkel Z 1979 *Phys. Rev. C* **20** 2227–2243

[10] Bertini H W 1963 *Phys. Rev.* **131**(4) 1801–1821
Bertini H W 1969 *Phys. Rev.* **188**(4) 1711–1730

[11] Villagrasa-Canton C *et al.* 2007 *Phys. Rev. C* **75** 044603

[12] Rejmund F, Mustapha B, Armbruster P *et al.* 2001 *Nucl. Phys. A* **683** 540–565

[13] Giot L, Alcántara-Núñez J A, Benlliure J *et al.* 2013 *Nucl. Phys. A* **899** 116–132

[14] Napolitani P, Schmidt K H, Tassan-Got L *et al.* 2007 *Phys. Rev. C* **76** 064609

[15] Audouin L, Tassan-Got L, Armbruster P *et al.* 2006 *Nucl. Phys. A* **768** 1–21

[16] Enqvist T, Wlazło W, Armbruster P *et al.* 2001 *Nucl. Phys. A* **686** 481–524

[17] Taïeb J, Schmidt K H, Tassan-Got L *et al.* 2003 *Nucl. Phys. A* **724** 413–430

[18] Titarenko Y E *et al.* 2002 Experimental and theoretical study of the yields of residual product nuclei produced in thin targets irradiated by 100–2600 MeV protons INDC report INDC(CCP)-434 IAEA, Nuclear Data Section, International Nuclear Data Committee URL `https://www-nds.iaea.org/publications/indc/indc-ccp-0434.pdf`

[19] Michel R, Gloris M, Lange H J *et al.* 1995 *Nucl. Instrum. Meth. B* **103** 183–222

[20] Reeder P L 1969 *Phys. Rev.* **178**(4) 1795–1801

[21] Blomqvist J and Wahlborn S 1960 *Ark. Fys.* **16**

[22] Chen C X, Albergo S, Caccia Z *et al.* 1997 *Phys. Rev. C* **56**(3) 1536–1543